



OPEN

SUBJECT AREAS:

BIOLOGICAL PHYSICS

COMPUTATIONAL MODELS

Received  
29 August 2013Accepted  
1 November 2013Published  
27 November 2013

Correspondence and requests for materials should be addressed to K.-H.C. (chiamkh@bii.a-star.edu.sg) or S.P. (nanopark@ewha.ac.kr)

# *C. elegans* sensing of and entrainment along obstacles require different neurons at different body locations

Seong-Won Nam<sup>1</sup>, Chen Qian<sup>2</sup>, So Hyun Kim<sup>1</sup>, Danny van Noort<sup>1</sup>, Keng-Hwee Chiam<sup>2,3</sup> & Sungsu Park<sup>1,2</sup>

<sup>1</sup>Department of Chemistry and Nano Science, Ewha Global Top5 Research Program, Ewha Womans University, Seoul, Korea, <sup>2</sup>Mechanobiology Institute (MBI), National University of Singapore, Singapore, <sup>3</sup>A\*STAR Bioinformatics Institute, Singapore.

We probe *C. elegans* mechanosensation using a microfabricated platform where worms encounter a linear array of asymmetric funnel-like barriers. We found that sensing of and moving along barriers require different sets of neurons located at different parts of the animal. Wild-type worms sense and move along the barrier walls, leading to their accumulation in one side of the barriers due to the barriers' asymmetric shape. However, *mec-4* and *mec-10* mutants deficient in touch sensory neurons in the body exhibited reversal movements at the walls, leading to no accumulation in either side of the barriers. In contrast, *osm-9* mutants deficient in touch sensory neurons in the nose, moved along the barrier walls. Thus, touch sensory neurons ALM and AVM in the body are required for *C. elegans* to sense and move along obstacles, whereas the ASH and FLP neurons in the nose are required only for sensing of but not moving along obstacles.

Nematodes play an important role in nutrient recycling by feeding on plants, bacteria, fungi, and other microscopic organisms. They move in the soil by propagating sinusoidal waves along their bodies and occasionally change their direction of movement either by transient reversals or by turning their heads during forward movement. While their movement is relatively well understood, how they sense, interact with, and respond to obstacles is not. Herein, we study the interplay between the physical and neuronal basis for nematode interaction with obstacles, i.e., how much of the nematode's sensing of and response to obstacles is governed physically and neuronally, and what specific neurons are used at various stages of this process. There have been previous studies on nematodes' dispersal abilities and how soil structure affects their movement<sup>1,2</sup>. However, these studies have traditionally been done on smooth agar plates coated with sand particles to create a structurally heterogeneous environment, or post arrays to create a structurally homogeneous environment<sup>1-4</sup>. Although these assays are useful for studying the effect of, say, inter-obstacle distance on the dispersal ability of the nematodes, it is not easy to interrogate the effects that other physical parameters may play in nematode mechanosensation.

The soil nematode *Caenorhabditis elegans* is often used to study how animal behavior is regulated by the underlying neuronal circuit because it has only 302 neurons<sup>5</sup>. Among the neurons, ASH, ALM, AVM, PVM, FLP, IL1 and OLQ have been shown to be associated with mechanosensory responses (Fig. 1A)<sup>5,6</sup>. However, these investigations typically rely on assays of behavioral responses to touch by either an eyelash hair attached to a toothpick or a platinum wire pick<sup>6-8</sup>. The results from these studies may not necessarily reflect the behavior of *C. elegans* in its soil habitat.

To allow us to study in combination the effects of both physical and neuronal sensing, we have developed a microfabricated platform to study *C. elegans* mechanosensation. In this assay, worms crawl freely on an agar surface until they encounter a linear array of asymmetric funnel-like barriers located on top surface of the agar (Fig. 1B). The asymmetry of the funnel-like barriers resulted in a difference in the gap spacing for a worm crawling from the left side of the barriers to the right, and vice versa. Therefore, if the persistence length of the crawling motion is longer than the gap spacing, then more worms will crawl from the side with the bigger gap spacing to the side with the smaller gap spacing, resulting in the accumulation of worms on the side of the barriers with the smaller gap spacing. We term this effect rectification. A similar device was previously used to study the rectification of swimming bacteria<sup>9-11</sup>. However, unlike worms, bacteria do not exhibit mechanosensation and hence their rectification can be explained using only physical arguments. In this study, we ask how higher organisms with neuronal circuitry respond in such an assay. In particular, we ask how much of the response is simply physical, and how much of it is neuronal, and what specific neurons are involved.

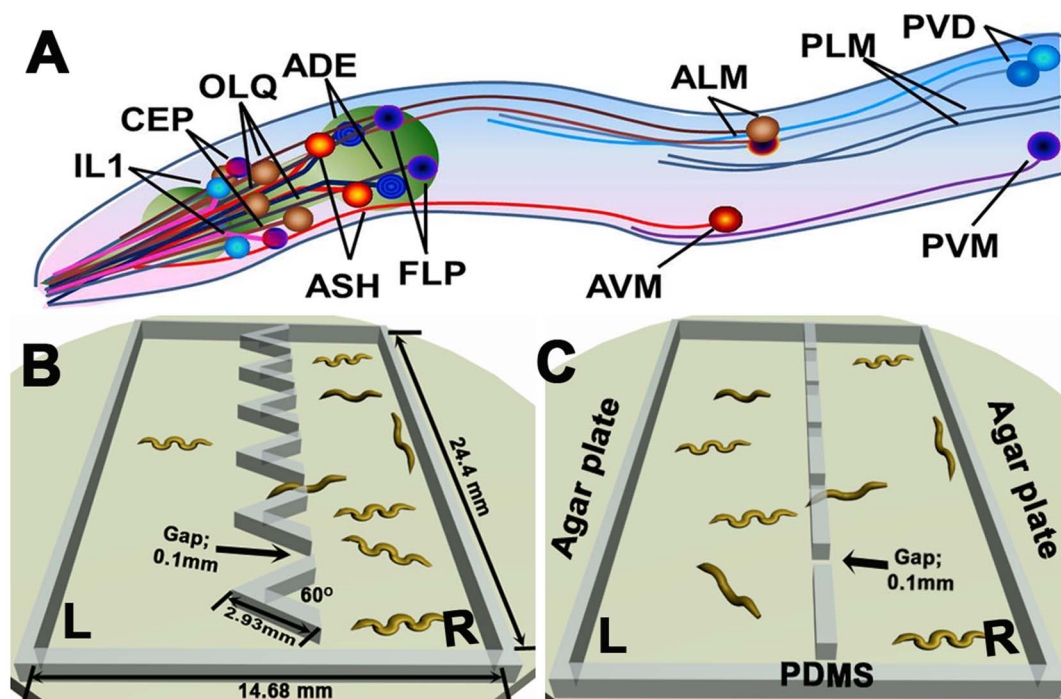


**Figure 1** | The microfabricated platform with the linear array of asymmetric funnel barriers in the middle used to study the rectification behavior of *C. elegans* wild-type N2. (A) Schematic drawing of the putative mechanosensory neurons on the anterior end and body (based on articles in the Wormbook<sup>25,26</sup>). (B) Schematic drawing of the experimental setup. *C. elegans* on an agar plate underwent rectification and became concentrated on the right side (labeled R) over time. (C) Schematic drawing of the control setup where the barriers are symmetric. In this case, there is no rectification and *C. elegans* were equally distributed between the left (L) and right (R) sides.

We showed that *C. elegans* wild-type (N2) and its mechanosensory-defective mutants (*mec-4* (e1339) and *mec-10* (e1515)) exhibit markedly different behaviors when interacting with the funnel walls, even though their morphologies and movements are identical<sup>3</sup>. Wild-type worms were entrained and crawled along the funnel walls whereas the *mec* worms reversed their directions upon encountering the walls. Thus, the wild-type worms, like swimming bacteria, accumulated on the side of the array with small gap spacing. However, *mec-4* and *mec-10* worms, which are deficient in touch sensory

neurons in the body<sup>12</sup>, did not. Thus, despite wild-type worms' similarity to swimming bacteria in terms of rectification behavior, the mechanisms for which they do so are fundamentally different.

We also developed a computational model of worm movement in the assay. The model was based on an earlier one<sup>10</sup>, but considered the worm-wall interactions more carefully. Our model showed that rectification depends on both the degree of asymmetry of the funnel barriers and the orientation of the worm to the barrier wall after their initial touch.

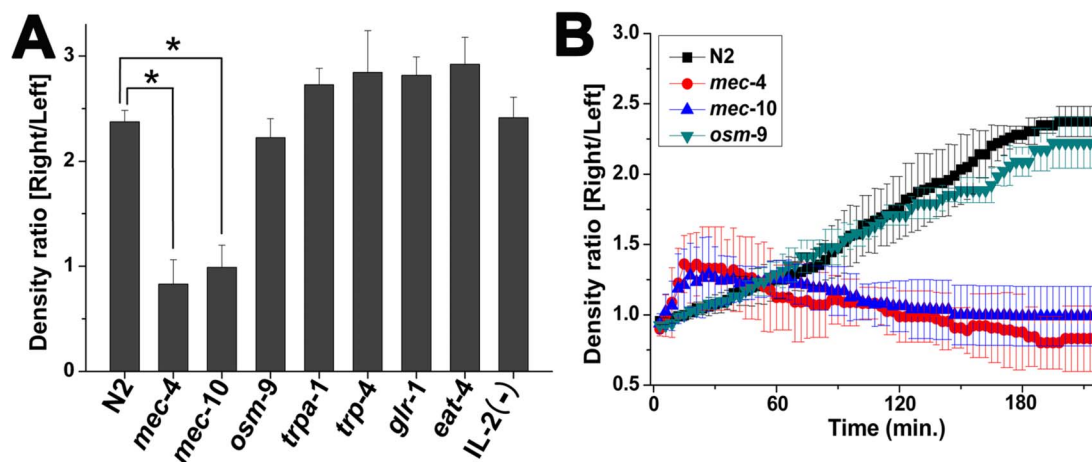


**Figure 2** | Comparison of the rectification behaviors of the wild-type N2 and its various mutants. (A) Ratio of the density of worms in the right to the left side of the funnels after 180 minutes. A high ratio indicates rectification, whereas a ratio close to unity indicates no rectification. Asterisks denote values that are different from the value of the wild-type N2 at  $p < 0.0001$  (One-way ANOVA with Bonferroni post-tests analysis). The ratios were plotted as the mean  $\pm$  standard deviation of 4 independent experiments (each experiment with 50–60 young adult worms, each worm of length between 0.7 mm and 0.8 mm long). (B) Density ratios as a function of time for the wild-type N2 and its *mec-4*, *mec-10* and *osm-9* mutants. The ratio was given as the mean  $\pm$  standard deviation of 4 independent experiments (each experiment with 50–60 young adult worms, each worm of length between 0.7 mm and 0.8 mm long).

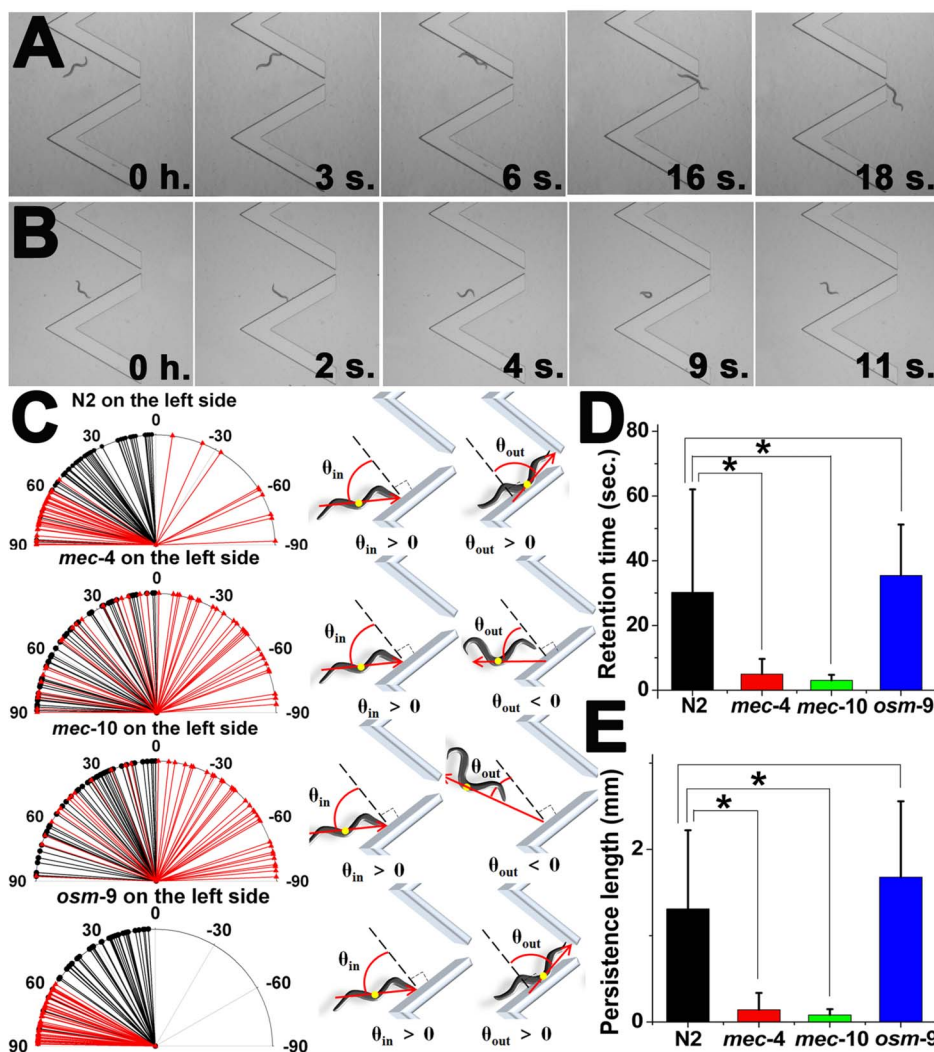


**Figure 3** | Representative images and behaviors of wild-type (N2) and mutants after colliding with a funnel wall. (A) Representative images of N2. (B) Representative images of *mec-4*. (C) Distribution of incoming and outgoing angles (incoming: black lines with circles, outgoing: red lines with triangles), as well as schematic drawings of several instances of incoming and outgoing angles. (D) Retention times on the funnel wall. (E) Persistence lengths on the funnel wall. Asterisks denote values that are different from the value of the wild-type N2 at  $p < 0.0001$  (One-way ANOVA with Bonferroni post-tests analysis). The values were plotted as the mean  $\pm$  standard deviation of 50 independent worm's movements after touching the wall.

## Results

**Asymmetric funnels rectify the wild-type worms.** About 50 to 60 worms were evenly distributed on both sides of the funnel array on the agar. Over time, the number of worms crawling from the side of the barriers with the large gap spacing (left, L) to the side with the small gap spacing (right, R) increased. After 180 min., the number of worms accumulating on the right side of the array became more than two times that of worms on the left side of the array. (Figs. 2A, S1A and S1B). Rectification was not observed (Figs. S1A and B) when worms were located in an enclosure with a linear array of symmetric barriers (Fig. 1C).

**Touch sensory neurons in the body contribute to worm rectification.** Among various types of mutants (Supplemental Table 1), *mec-4* and *mec-10* did not exhibit rectification (Figs. 2A and B). However, unexpectedly, the nose-touch-insensitive mutant *osm-9*<sup>13</sup> did exhibit rectification to a similar extent as wild-type.

**Wild-type worms entrain along the funnel wall but the *mec* mutants do not.** Upon bumping into the funnel walls, most of wild-type worms first exhibited repeated forward and backward movements, but eventually moved along the walls, irrespective of their incoming

angles toward the walls (Movie S1 and Fig. 3A). In contrast, *mec-4* and *mec-10* did not exhibit entrainment along the walls. Instead, they either retracted from the walls (Movie S2), or reversed their directions via omega turns (Fig. 3B). Omega turns were identified by the head nearly touching the tail or a reorientation of more than  $135^\circ$  within a single head swing<sup>14</sup>.

Fig. 3C showed that the incoming angles of wild-type worms at a wall ranged from  $0^\circ$ , corresponding to a worm hitting the wall perpendicularly, to  $90^\circ$ , corresponding to a worm hitting the wall in a parallel manner. The outgoing angles mostly ranged between  $60^\circ$  and  $90^\circ$ . (Several worms also displayed negative outgoing angles ranging from  $0^\circ$  to  $-90^\circ$ , which indicate reversals in the trajectories.) Thus, most of wild-type worms moved parallel to the walls after bumping into them, irrespective of the incoming angle toward the wall. On the other hand, the incoming angles of the *mec* mutants, while also ranging from  $0^\circ$  to  $90^\circ$ , instead displayed outgoing angles that were negative (Fig. 3C). This indicated that they were not entrained along the funnel walls, but instead reversed their directions when they hit the walls. Interestingly, *osm-9* did not display negative outgoing angles, indicating that it did not show any reversal movements. Instead, it behaved just like wild-type.

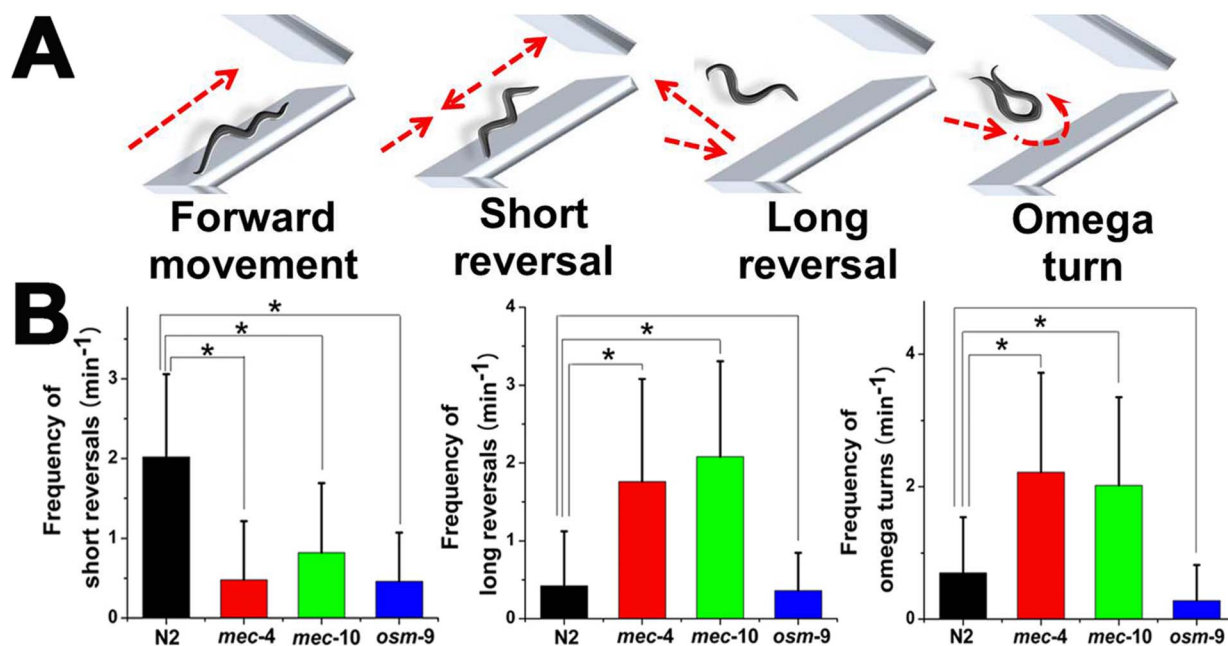


**Figure 4** | Comparison of reversal movements of the wild-type N2 and its mutants. (A) Schematic drawing of the four types of responses after colliding with a wall. (B) Frequency of short reversals, long reversals, and omega turns after touching the wall. Asterisks denote values that are different from the value of the wild-type N2 at  $p < 0.0001$  (One-way ANOVA with Bonferroni post-tests analysis). Frequencies were given as the mean  $\pm$  standard deviation of 50 independent experiments. Significant difference was calculated with one-way analysis of variance (ANOVA) with Bonferroni post-tests.

The retention times and persistence lengths of the worms were also measured. The retention time is defined as the duration that a worm spent while crawling along the funnel wall. The retention times of both wild-type and *osm-9* were significantly longer than those of *mec-4* and *mec-10* (Fig. 3D). The persistence length is defined as the length of a worm's trajectory along the funnel wall, with at least the anterior and posterior touching the wall, and without any reversal or change in orientation. The persistence lengths of wild-type and *osm-9* were longer than those of *mec-4* and *mec-10* (Fig. 3E). Once wild-type and *osm-9* worms were entrained along the funnel walls, they usually crawled in a straight line along the wall for about 2 mm before changing directions, which is comparable to the length of funnel walls, namely 2.93 mm. In contrast, both *mec-4* and *mec-10* worms exhibited higher frequencies of long reversals and omega turns than wild-type and *osm-9* worms did (Fig. 4B).

**Degenerin/Na<sup>+</sup> channels are required for wall entrainment.** The *mec-4* and *mec-10* genes encode their respective subunits of a mechanically-gated degenerin/Na<sup>+</sup> channel in the touch sensory neurons in the body<sup>12,15–18</sup>. In order to elucidate whether the mutated degenerin/Na<sup>+</sup> channels are responsible for the lack of wall entrainment and reversal at the walls, the *mec* mutants were treated with amiloride, a degenerin/Na<sup>+</sup> channel blocker<sup>16</sup>. After incubation with 0.3 mM amiloride for 14 hrs, *mec-4* and *mec-10* exhibited rectification, just like wild-type (Fig. 5A).

**Computational model shows wall entrainment is necessary for rectification.** We represent the worms by their centroids and assume that each centroid moves as a point particle subject to a drag force, a motility force arising from the worm's undulatory propulsion, and a repulsive force that represents the interaction between the worm and the funnel walls. The motility force has a persistent length associated with the worm's persistent crawling. The repulsive force is non-zero only when the worm is near to the wall. To simulate the near-wall behavior of the worms, the vectorial direction of the interaction force is changed when a worm first touches the wall. The reoriented direction is decided by the distribution of the incoming

and outgoing angles at the wall as measured experimentally (Fig. 3C).

From the simulations, representative trajectories of wild-type and *mec-4* worms are shown in Fig. 6B and 6C, respectively. The rectification for wild-type increased with time while *mec-4* did not present such an effect (Fig. 6A), consistent with experimental results (Fig. 2B). The simulated trajectories are not deterministic, because they incorporate randomness in the form of reorientations at the wall, and thus, they also reflect the randomness observed in the experiments.

Wild-type and *mec-4* represent the two extremities of the range of possible worm-wall interaction: the former exhibiting wall entrainment (outgoing angle around 0° measured from the wall to the normal) and the latter showing complete reversal, with no wall entrainment (outgoing angle around 90°). We therefore used the simulation to predict how an intermediate value of outgoing angle between 0° and 180° would affect rectification. We observed that there exists a threshold outgoing angle below which no rectification would occur, and that this threshold depends on the asymmetry of the funnel barriers as measured by the half-angle between the two arms of the V-shaped funnels (Fig. 7A). The presence of such a threshold outgoing angle can be attributed to the fact that the crawling persistent length is very much longer than the barrier and gap sizes and thus, a smaller outgoing angle would geometrically lead to the worm's trajectory being "reflected" back into the side of array that has the larger gap spacing (Fig. 7B). For the 30° funnels used in this study, the threshold outgoing angle is between 40°–50° (Fig. 7C). Thus, given a particular strain of a worm that has a characteristic outgoing angle, rectification can only occur if the funnels are of a particular geometry. As an example, we simulated 50° funnels and found that rectification is reduced (Fig. 7D). Indeed, for very narrow (close to 0°) or very wide funnels (close to 90°) where the degree of asymmetry is reduced, the threshold outgoing angle approaches 0°, indicating no rectification, as is to be expected theoretically. Therefore, we conclude that worm wall entrainment is a combination of both physical (as determined by the funnel geometry and crawling persistent length) and neuronal (as determined by the outgoing angle) effects.

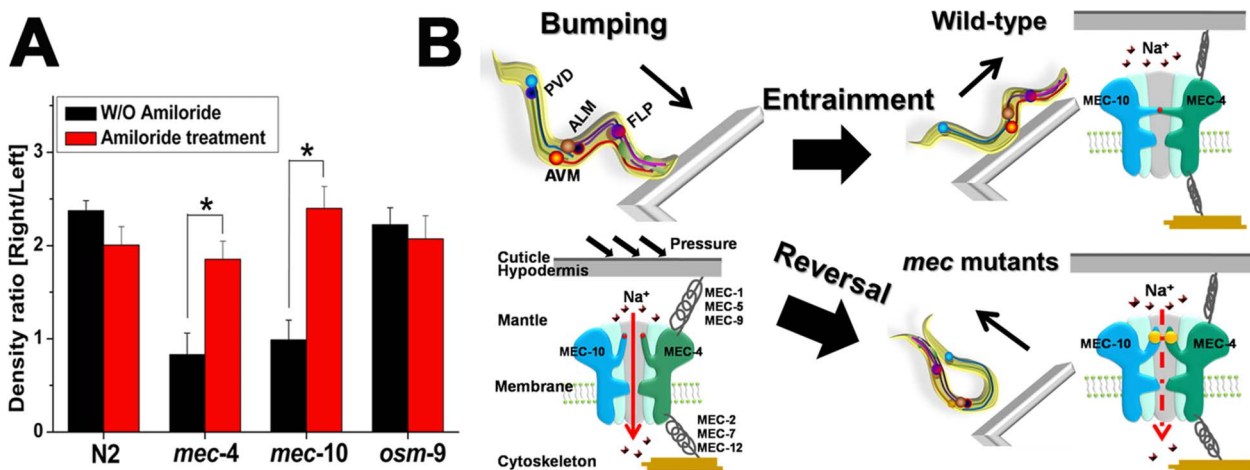


**Figure 5 | Relation between degenerin/Na<sup>+</sup> channel and rectification behavior of *C. elegans*.** (A) Effect of degenerin/Na<sup>+</sup> channel blocker, amiloride, on the density ratio after 180 min. Asterisks denote values that are different from the value of *mec-4* and *mec-10* without treatment of amiloride at  $p < 0.0001$  (One-way ANOVA with Bonferroni post-tests analysis). The ratio was given as the mean  $\pm$  standard deviation (s.d.) of 4 independent experiments (each experiment with 50–60 young adult worms, each worm of length between 0.7 mm and 0.8 mm long). (B) Schematic drawing of the putative relationship between degenerin/Na<sup>+</sup> channel and rectification behavior of *C. elegans*.

**Worms overcome rectification in the presence of food.** When a drop of bacterial culture of *Escherichia coli* OP50 was placed to the left side of the funnel array, worms on the right side of the array started to crawl across the array to reach the food source. Eventually, they aggregated on the left side, particularly at the location of the food (supporting information Fig. S3). This result is true for all the tested strains except *mec-10*.

## Discussion

Upon bumping into the obstacles, most of wild-type worms first exhibited repeated forward and backward movements without allowing their posterior part to touch the wall, until they were entrained and started to move along the wall (Movie S1 and Fig. 3A). *mec-4* and *mec-10* worms were not entrained due to their frequent reversal behaviors (short, long, and omega turns, etc). Among the anterior mechanosensory neurons (Fig. 1A), the *mec-4* gene is expressed in ALM and AVM, while the *mec-10* gene is expressed in ALM, AVM and FLP. Therefore, it is suggested that the mechanosensory neurons (ALM and AVM) on the anterior body part are required for a worm to be entrained along the funnel wall.

The hyperactivity of the degenerin/Na<sup>+</sup> channel in *mec-4* and *mec-10* worms is responsible for the frequent reversal behaviors of these worms upon bumping into the wall. The *mec-4* and *mec-10* genes encode subunits of amiloride-sensitive Na<sup>+</sup> ion channels of the degenerin/epithelial sodium channel (DEG/ENaC) family that form the pore of the channel complex (Fig. 5B)<sup>12</sup>. The mutation of these subunits induces the hyperactivation of the neurons<sup>16</sup>. The hyperactivation is caused by conformational changes to the channel, which might induce aberrant closing of the degenerin/Na<sup>+</sup> channel<sup>12</sup>. In the presence of amiloride, which binds and blocks the degenerin/Na<sup>+</sup> channel, the *mec* mutants exhibited rectification (Fig. 5A), suggesting that the hyperactivation of the degenerin/Na<sup>+</sup> channel upon bumping into the funnel wall is suppressed by amiloride.

The nose touch neurons such as ASH and FLP are required only for probing obstacles, but not for wall entrainment and rectification. Worms touched their nose to the wall at first (supporting information Movies S1, S2). The nose-touch-insensitive mutants, *osm-9*, *trpa-1*, and *trp-4* with mutated TRP ion channels and IL-2 (–) exhibited rectification, just like the wild-type worms (Fig. 2). However, unlike other nose-touch-insensitive mutants, *osm-9* showed reduced short reversal movements compared to wild-type (Fig. 4). It is known that the *osm-9* gene is expressed in the ciliated

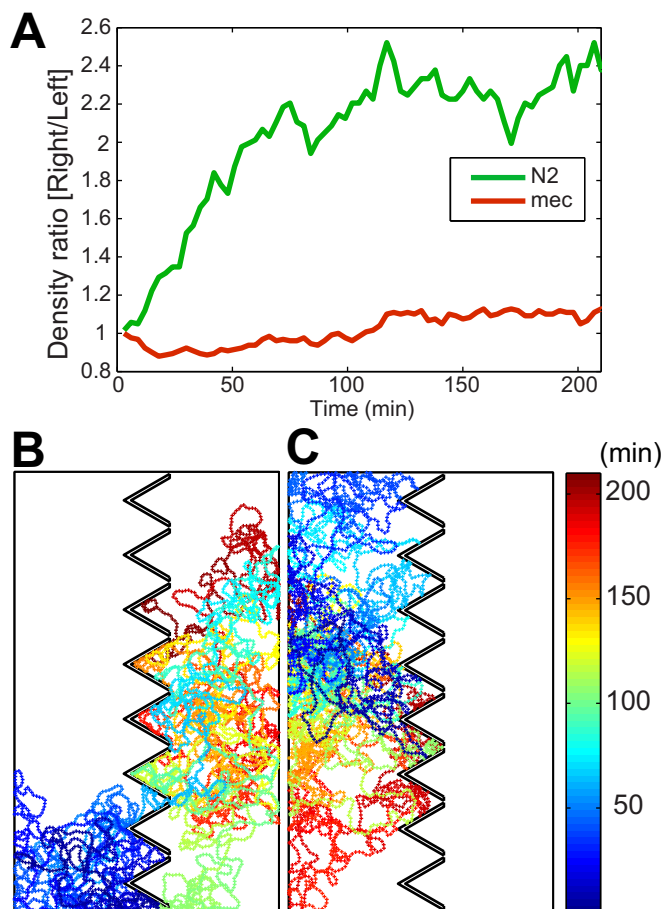


**Figure 6 | The rectification of wild-type and *mec-4* worms obtained from computational modeling.** (A) Ratio of the density of worms in the right side of the funnels to all the worms in the chamber as a function of time. The ratios are averaged from 10 simulations, each of 50 worms and for 210 min. (B) Representative trajectory of a N2 worm. Color codes for time (blue: early; red: late). (C) Representative trajectory of a *mec-4* mutant.

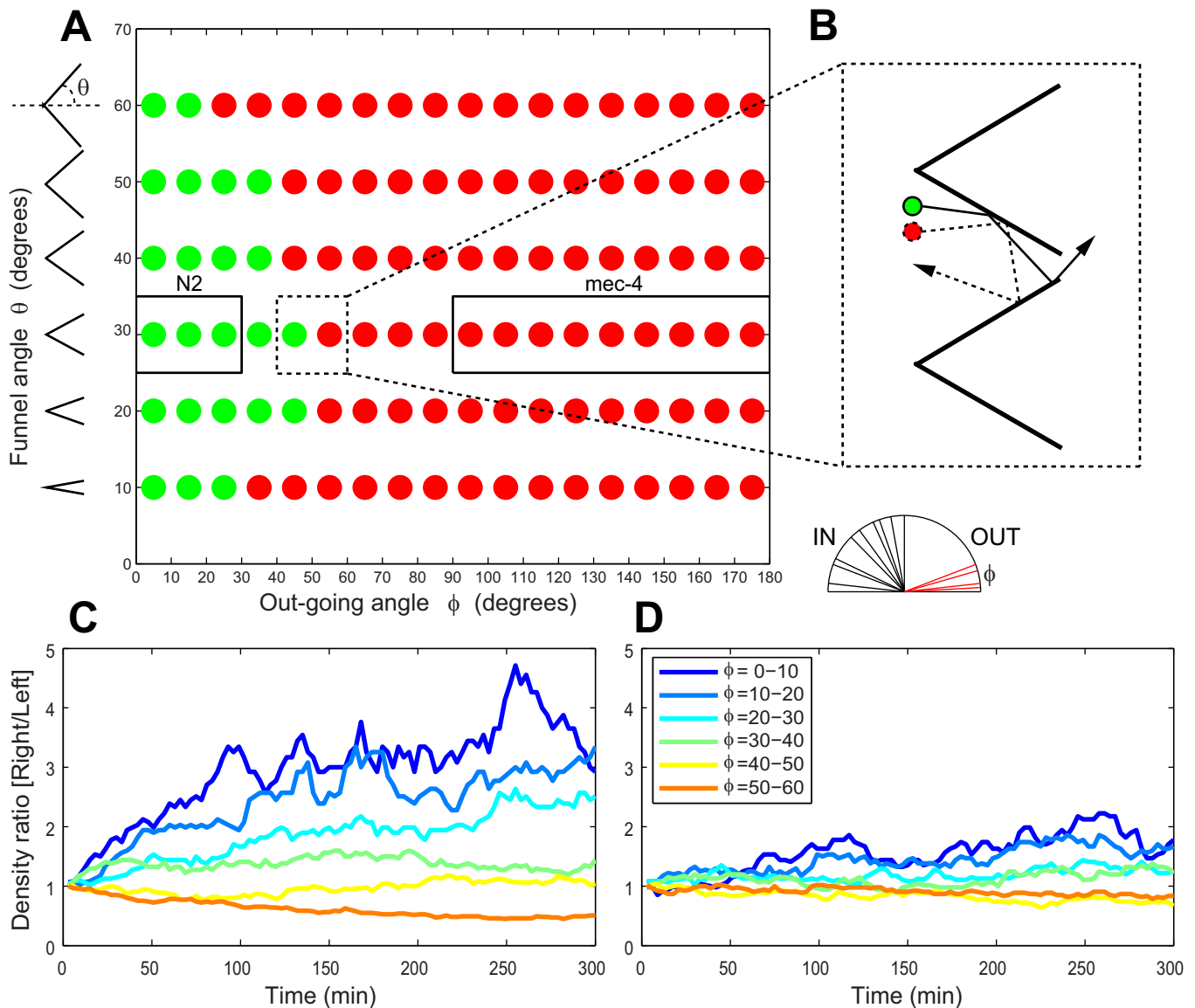


**Figure 7 | Rectification or no rectification as predicted from the computational modeling for different near-wall behaviors and for different funnel geometries.** (A) Green dots indicate rectification and red dots indicate no rectification. The  $x$ -axis is the outgoing angle the worms adopt upon leaving the walls. The  $y$ -axis is the half-angle between the two arms of the funnel walls as illustrated. Rectification is defined if the average of the density ratio at the steady-state level (after 100 min.) is above 1. (B) Illustration showing the geometrical argument why smaller outgoing angle results in rectification but bigger outgoing angles do not. A worm with small outgoing angles (green and solid line) may encounter multiple barriers without changing its overall direction. A worm with bigger outgoing angles (red and dotted line) may encounter multiple barriers but because of the large outgoing angle, the worm may hit the second barrier in a way that results in “reflected” movement after the second encounter. (C, D) Density ratio of worms in funnels of  $\theta = 30^\circ$  and funnels of  $\theta = 50^\circ$  respectively. The ratios are averaged from 4 simulations each having 50 worms. The outgoing angles are color coded as shown in the legend.

ASH sensory neuron<sup>13</sup>, and ASH is required for the avoidance response when the nose is touched<sup>7</sup>. It was also suggested that ASH as a polymodal sensory neuron is a functional analogue to nociceptors related to the sensation of pain<sup>19,20</sup>. After colliding with the funnel walls, *osm-9* showed some reduction of the crawling length and speed, while wild-type showed more significant reduction of the migration length and speed (supporting information Fig. S2). The reduced migration length and speed of wild-type were due to repeated short reversals and forward movements while crawling on the wall (supporting information Movie S1). The purpose of the repeated touching and reversal seems to be to inspect the physical barrier. Since *osm-9* lacks this behavior, it is suggested that ASH is a critical neuron for this behavior. When it is presumed that the modest reversal behaviors in wild-type are the natural behavior for a

worm to probe the physical structure of obstacles until it figures out the structure, the disappearance of the reversal behaviors in *osm-9* may not be advantageous for the worm in surviving in the soil.

Another interesting result was that wild-type as well as *mec-4* could overcome the physical asymmetry of the funnels in the presence of food (supporting information Fig. S3), while *mec-10* hardly reached the food source (supporting information Fig. S3). Unlike the *mec-4* gene, which is only expressed on body-touch neurons, the *mec-10* gene is not only expressed in body-touch neurons, but also in FLP and PVD neurons<sup>12</sup>. Therefore, the *mec-10* mutation might have induced more severe defects in rectification behavior than *mec-4* mutation, and thus *mec-10* could not overcome the physical barrier of the funnel, even in the presence of food.



Many habituation studies have been performed using the tap stimuli of a plate<sup>21</sup>. However the assay may bring difficulties in finding the direct correlation between the stimuli and the underlying neuronal circuitry. We found that rectification can only be achieved when the worms are sufficiently entrained by the walls. We speculate that this behavior has evolved due to frequent encounters with obstacles in the worm's natural habitat. It will thus be interesting to validate whether the worms habituate to the mechanosensory stimuli induced by the funnel walls and whether they evade (i.e., do not exhibit rectification) under some conditions, and to test which neurons are related to the habituation.

It is concluded that ALM and AVM neurons on the body are the most critical mechanosensory neurons for this entrainment and rectification. However, we cannot rule out the possibility that the mechanosensory neurons on the posterior body (PVM and PLM) are also involved in this behavior, in part as the force induced by touching the wall at the anterior end might be passed on through the body to the posterior end. The microfabricated platform can be used not only for the study of mechanosensory behaviors but also for the study of chemotaxis, habituation and ecological behaviors of nematodes.

## Methods

**C. elegans strains and growth.** All the strains (Supplemental Table 1) except IL-2 (–) were obtained from the *Caenorhabditis* Genetics Center. The IL-2 (–) strain was obtained from Junho Lee<sup>22</sup>. Worms were grown and maintained as described in Brenner<sup>23</sup>. Only young adults (0.7–0.8 mm long) were selected for the experiments.

**Funnel fabrication.** Soft lithography<sup>24</sup> was used to a thin rectangular enclosure (14.68 mm by 24.4 mm) made of poly(dimethyl siloxane) (PDMS), which were divided into two halves (7.34 mm by 24.4 mm) by an array of 8 funnel-like structures. The sides of the funnels were 2.93 mm and formed at a 60° angle<sup>9</sup>. The gaps between adjacent funnels were 100 μm wide. The funnel-like structure and frame were 105 μm deep.

**Rectification behavioral assay.** Worms were collected in NGM buffer and washed 3× with NGM buffer<sup>23</sup>. Two drops (about 50 μL) containing 50–60 worms were placed approximately 7 cm apart in the center region of an NGM agar plate without *E. coli* OP50 and the microfabricated funnel-like barriers was then located between the drops by carefully covering the PDMS enclosure into the plate. Observation started to be made when the water on the drops was evaporated and the worms started to crawl. Sequential images (1 frame/sec.) were taken under a stereoscope (SMZ1500; Nikon) with a peltier-cooled CCD camera (Spot Insight 4; Diagnostic Instruments Inc., Sterling Heights, MI), and analysis was performed with MATLAB software (The Mathworks Inc., Natick, MA) or by counting *C. elegans*.

**Computational modeling.** The location of the *i*-th worm at time *t* is represented by the coordinates of its centroid  $\mathbf{R}_i(t)$ . We assume that the worm, represented by its centroid, is acted on by three distinct forces: the drag force  $-\eta d\mathbf{R}_i/dt$  as the worm crawls on the agar plate ( $\eta$  being the drag coefficient), the motility force  $\mathbf{F}_i^M(t)$  arising from the worm's undulatory propulsion, and the repulsive force  $\mathbf{F}_i^R$  that represents the interaction between the worm and the funnel walls and is non-zero only when the worm is in close contact with the walls. Therefore, the equation of motion for the worm's centroid is

$$\eta d\mathbf{R}_i/dt = \mathbf{F}_i^M(t) + \mathbf{F}_i^W$$

which we can integrate numerically to obtain the trajectory  $\mathbf{R}_i$  as a function of time. Inertial effects are neglected due to the low Reynolds numbers associated with worm crawling. A worm can be crawling in free space or "on the wall" when it is within a distance of 0.02 mm to the wall. The magnitude of  $\mathbf{F}_i^M(t)/\eta$  (which has unit of speed) is chosen such that for each worm, its speed in free space and on the wall follow the experimentally measured values (Supplemental Table 2). The vectorial direction of  $\mathbf{F}_i^M$  changes by a small amount after each time step to model the fact the worms crawl with a persistent length (Supplemental Table 2). Upon hitting a wall,  $\mathbf{F}_i^M(t)$  changes its orientation. For wild-type worms, the outgoing angle mostly aligns with the barrier wall, with outgoing angles chosen uniformly from 0° to 30°. For the *mec* mutants, the outgoing angle is bigger than 90°, which means that the worm retracts from the barrier with the outgoing angle chosen uniformly from 90° to 180°. The repulsive force  $\mathbf{F}_i^W$  is non-zero only when the worm is on the wall, and decays when the worm moves away from the wall, namely

$$|\mathbf{F}_i^W| = f_w \times (r_w - d)/r_w$$

where *d* is the distance of the centroid from the worm to the wall,  $r_w = 0.02$  mm, and  $f_w$  is a constant. The direction of  $\mathbf{F}_i^W$  is set to be perpendicular to and away from the wall. To simulate the near-wall behavior of the worms, we reoriented the vectorial

direction of  $\mathbf{R}_i$  when a first touches the wall. The reoriented direction is decided by the distribution of the incoming and outgoing angles at the wall as measured experimentally (Fig. 3C). In the simulations, we set  $|\mathbf{F}_i^W| = |\mathbf{F}_i^M|$ .

**Statistical analysis.** The data are reported as bar graphs that include every data point of *n* independent experiments, with 50 to 60 or 30 to 40 animals for each experiment. A significant difference was calculated with one-way analysis of variance (ANOVA) with Bonferroni post-tests, and defined as  $p < 0.05$  using an unpaired two-tailed *t* test (Graphpad, La Jolla, CA).

- Anderson, A. R., Young, I. M., Sleeman, B. D., Griffiths, B. S. & Robertson, W. M. Nematode movement along a chemical gradient in a structurally heterogeneous environment. 1. Experiment. *Fund. Appl. Nematol.* **20**, 157–163 (1997).
- Hapca, S., Budha, P., Crawford, J. & Young, I. Movement of the nematode, *Phasmarhabditis hermaphrodita*, in a structurally heterogeneous environment. *Nematology* **9**, 731–738 (2007).
- Park, S. *et al.* Enhanced *Caenorhabditis elegans* locomotion in a structured microfluidic environment. *PLoS One* **3**, e2550 (2008).
- Johari, S., Nock, V., Alkai, M. M. & Wang, W. On-chip analysis of *C. elegans* muscular forces and locomotion patterns in microstructured environments. *Lab Chip* **13**, 1699–707 (2013).
- Bargmann, C. I. & Kaplan, J. M. Signal transduction in the *Caenorhabditis elegans* nervous system. *Annu. Rev. Neurosci.* **21**, 279–308 (1998).
- Chalfie, M. *et al.* The neural circuit for touch sensitivity in *Caenorhabditis elegans*. *The Journal of neuroscience* **5**, 956–64 (1985).
- Kaplan, J. M. & Horvitz, H. R. A dual mechanosensory and chemosensory neuron in *Caenorhabditis elegans*. *Proc. Natl. Acad. Sci. USA.* **90**, 2227–31 (1993).
- Li, W., Kang, L., Piggott, B. J., Feng, Z. & Xu, X. Z. S. The neural circuits and sensory channels mediating harsh touch sensation in *Caenorhabditis elegans*. *Nat. Commun.* **2**, 315 (2011).
- Galajda, P., Keymer, J. E., Chaikin, P. & Austin, R. H. A wall of funnels concentrates swimming bacteria. *J. Bacteriol.* **189**, 8704–7 (2007).
- Wan, M., Olson Reichhardt, C., Nussinov, Z. & Reichhardt, C. Rectification of Swimming Bacteria and Self-Driven Particle Systems by Arrays of Asymmetric Barriers. *Phys. Rev. Lett.* **101**, 1–4 (2008).
- Tailleur, J. & Cates, M. E. Sedimentation, trapping, and rectification of dilute bacteria. *Europhys. Lett.* **86**, 60002 (2009).
- Syntichaki, P. & Tavernarakis, N. Genetic models of mechanotransduction: the nematode *Caenorhabditis elegans*. *Physiol. Rev.* **84**, 1097–153 (2004).
- Tobin, D. M. *et al.* Combinatorial Expression of TRPV Channel Proteins Defines Their Sensory Functions and Subcellular Localization in *C. elegans* Neurons. *Neuron.* **35**, 307–18 (2002).
- Gray, J. M., Hill, J. J. & Bargmann, C. I. A circuit for navigation in *Caenorhabditis elegans*. *Proc. Natl. Acad. Sci. USA.* **102**, 3184–91 (2005).
- Adams, C. M., Snyder, P. M., Price, M. P. & Welsh, M. J. Protons activate brain Na<sup>+</sup> channel 1 by inducing a conformational change that exposes a residue associated with neurodegeneration. *J. Biol. Chem.* **273**, 30204–7 (1998).
- García-Añoveros, J., García, J. A., Liu, J. D. & Corey, D. P. The nematode degeneration UNC-105 forms ion channels that are activated by degeneration-or hypercontraction-causing mutations. *Neuron.* **20**, 1231–41 (1998).
- Hong, K., Mano, I. & Driscoll, M. In vivo structure-function analyses of *Caenorhabditis elegans* MEC-4, a candidate mechanosensory ion channel subunit. *J. Neurosci.* **20**, 2575–88 (2000).
- Goodman, M. B. *et al.* MEC-2 regulates *C. elegans* DEG/ENAC channels needed for mechanosensation. *Nature.* **415**, 1039–42 (2002).
- Liedtke, W., Tobin, D. M., Bargmann, C. I. & Friedman, J. M. Mammalian TRPV4 (VR-OAC) directs behavioral responses to osmotic and mechanical stimuli in *Caenorhabditis elegans*. *Proc. Natl. Acad. Sci. USA.* **100** Suppl, 14531–6 (2003).
- Kindt, K. S. *et al.* *Caenorhabditis elegans* TRPA-1 functions in mechanosensation. *Nat. Neurosci.* **10**, 568–77 (2007).
- Rankin, C. H., Gannon, T. & Wicks, S. R. Developmental analysis of habituation in the nematode *C. elegans*. *Dev. Psychobiol.* **36**, 261–70 (2000).
- Lee, H. *et al.* Nictation, a dispersal behavior of the nematode *Caenorhabditis elegans*, is regulated by IL2 neurons. *Nat. Neurosci.* **15**, 107–12 (2012).
- Brenner, S. The genetics of *Caenorhabditis elegans*. *Genetics.* **77**, 71–94 (1974).
- Xia, Y. & Whitesides, G. M. Soft lithography. *Annu. Rev. Mater. Sci.* **28**, 153–184 (1998).
- Goodman, M. B. Mechanosensation (January 6, 2006), *WormBook*, ed. The *C. elegans* Research Community, <http://dx.doi.org/10.1895/wormbook.1.62.1>.
- Inglis, P. N., Ou, G., Leroux, M. R. & Scholey, J. M. The sensory cilia of *Caenorhabditis elegans* (March 8, 2007), *WormBook*, ed. The *C. elegans* Research Community, <http://dx.doi.org/10.1895/wormbook.1.126.2>.

## Acknowledgments

We thank J. Lee, S.-K. Lee, M.-k. Choi, D. Lee, and H. Hwang for comments, support and discussion. This work was equally supported by grants from the National Research Foundation of Korea (NRF) (Grant# 2012012221: Public Welfare & Safety Research Program #2012M3A2A1051681) and seed funds from the Mechanobiology Institute



financed by the National Research Foundation of Singapore and the Singapore Ministry of Education. The first author was supported by a 2012 Research Program Grant from Ewha Womans University.

### Author contributions

S.-W.N., S.H.K., D.v.N. and S.P. conducted experiments. C.Q. and K.-H.C. conducted simulations. S.-W.N., C.Q., K.-H.C. and S.P. wrote the manuscript. All authors reviewed and approved the manuscript.

### Additional information

**Supplementary information** accompanies this paper at <http://www.nature.com/scientificreports>

**Competing financial interests:** The authors declare no competing financial interests.

**How to cite this article:** Nam, S.-W. *et al.* *C. elegans* sensing of and entrainment along obstacles require different neurons at different body locations. *Sci. Rep.* 3, 3247; DOI:10.1038/srep03247 (2013).



This work is licensed under a Creative Commons Attribution-NonCommercial-NoDerivs 3.0 Unported license. To view a copy of this license, visit <http://creativecommons.org/licenses/by-nc-nd/3.0>